POSSIBLE STIMULATED AKR OBSERVED IN GALILEO, DE-1 AND POLAR WIDEBAND DATA

J. D. Menietti*, H. K. Wong†, W. S. Kurth*,
D. A. Gurnett*, L. J. Granroth* and J. B. Groene*

Abstract

The Galileo spacecraft observed intense auroral kilometric radiation during the second Earth encounter in 1992. High spectral resolution plots obtained by the wideband receiver of the plasma wave instrument on board the spacecraft often show discrete, negative-slope features each extending over a period of several seconds. Similar signatures are observed also in the DE-1 and Polar satellite wideband data. To date the features seem to be most commonly observed over the polar cap in a frequency range of 40 kHz $<$ f $<$ 100 kHz, but we cannot rule out observations of signatures at higher frequency. The frequency drift rates, R, are in the range -9.0 kHz/sec $<$ R $<$ -4.5 kHz/sec. A few cases of positive-slope features have been observed in the Polar data, and these show smaller frequency extents but larger drift rates in the range of 13 kHz/sec $<$ R $<$ 20 kHz/sec. The paucity of positive-slope features may be due to the location of the satellite at altitudes well above the AKR source region. We present evidence that suggests these features are due to AKR wave growth stimulated by the propagation of electromagnetic ion cyclotron waves travelling up ($-$R) or down (+R) the field line, through the source region.

1 Background

Gurnett et al. [1979c] and Gurnett and Anderson [1981] using ISEE data, Benson et al. [1988b] using DE-1 data, and Morioka et al. [1981] with EXOS-B data have all reported examples of auroral kilometric radiation (AKR) fine structure in both the ordinary and extraordinary modes indicating that AKR is emitted in discrete bursts lasting only a few seconds or less. Observed frequency drift rates of features are in the range 100 Hz/sec $<$ R $<$ 10s of kHz/sec.

Gurnett et al. [1979c] suggest that the drifting features may be due to rising and falling source regions. The fine structures include not only drifting features, but also discrete

*Dept. of Physics and Astronomy, U. of Iowa, Iowa City, IA 52242, USA
†Aurora Sciences Inc., 4502 Centerview Drive, San Antonio, TX 78228, USA

bands of near-monochromatic emission and other discrete features that are seen at the highest resolution available. Auroral roar is a relatively narrowband emission occurring near twice the electron gyrofrequency and first detected by Kellogg and Monson [1979]. While ground-based observations of auroral radio emissions have been reported in the past [Benson et al., 1988a], most recently LaBelle et al. [1995] and Shepherd et al. [this volume] have reported similar structures in auroral roar emissions at frequencies of a few MHz (2 or 3 times the local gyrofrequency). The signatures include a series of "multiple discrete features" with positive slope on a frequency-time spectrogram. These signatures are similar to those described by Menietti et al. [1996] in the AKR fine structure as "stripes", and postulated as stimulated emission. The relationship, if any, between the auroral roar discrete signatures and the AKR stripes is not known.

There are a number of theories that attempt to explain the source of the AKR fine structure observed. Such knowledge is necessary if we are to fully understand the details of the AKR generation mechanism. Wu and Lee [1979] have no doubt identified the general instability mechanism responsible for the emission, but as pointed out some years ago by Melrose [1986], the cyclotron maser mechanism would be an incomplete theory if it could not explain the time scales of wave growth associated with AKR fine structure.

Calvert [1982, 1981b, 1985] has proposed that AKR fine structure can be explained by a feedback model, which requires radiation oscillations (similar to an optical laser) in a density enhancement region of diameter ≤ 25 km that converges with altitude. The source would emit radiation at its normal modes and would thus naturally explain monochromatic fine structure bands. Fine structure features that are observed to drift in frequency are explained in the feedback model by density gradients at the boundaries of the density enhancement region. Melrose [1986] has proposed a feedback model that depends on a phase-bunching mechanism, and the wave trapping saturation model of VLF emission growth put forth by Helliwell [1967]. Melrose's theory of AKR fine structure depends critically on the assumption that the particle-wave interaction region for AKR growth has a parallel velocity intermediate between those of the particles and the waves. Occasional monochromatic signatures including bands of emission have been observed in the AKR fine structure. Grabbe [1982] presents examples of the latter features which he explains in terms of a three wave generation mechanism based on ion cyclotron waves [Grabbe et al. 1980]. Farrell [1995] has recently suggested that some monochromatic features in the AKR fine structure can be explained by free-energy electrons interacting with an oscillating density cavity boundary that has quasi-monochromatic wave-like motion. Adiabatic changes in the structure of the cavity can lead to drifting radio tones similar to those observed.

McKean and Winglee [1991] have performed 1-d P-I-C simulations of AKR fine-structure from sources associated with strong magnetic field gradients due to currents thought to be near or along the source field line. These authors find that rapidly drifting features (>10 kHz/sec) are proportional to the growth rate (for positive drift rate) or nearly constant (for negative drift rate). For slowly drifting features (close to observed drifts) the rates are approximately proportional to the B-field gradient.

Understanding the source of AKR fine structure is critical to understanding details of the generation mechanism. The frequency extent of the fine structure, for instance, puts se-

vere constraints on spatial growth rates as produced by the cyclotron maser instability. As mentioned above, Menietti et al. [1996] have presented observations of possible stimulated AKR. In that paper impulsive wave generation and intrinsic velocity dispersion was discounted as a possible source of the discrete signatures observed in the wave data. In this paper we extend the work of Menietti et al. by presenting additional observations of the phenomena observed by Polar and present a scenario for the generation of positive-slope signatures.

2 Observations

Galileo approached the Earth from the evening sector where it observed intense AKR. The observations we report were made when Galileo was approximately 10 to 12 R_E distant from Earth. In Figure 1 we present a frequency-time spectrogram of the plasma wave data obtained by the low, medium, and high-frequency receivers of the Plasma Wave System on board Galileo. The wave intensity is gray-coded with the most intense emissions appearing as black. The data were taken on December 8, 1992, prior to closest approach, CA. The intense AKR is seen in the figure to extend in frequency from about 50 kHz to over 600 kHz in the time interval from 08:00 UT to about 14:30 UT.

In Figure 2 we display a frequency-time spectrogram of the wideband data for a one-minute time period beginning at 13:07:04. The frequency range of the plot is from 40 to 80 kHz. Seen in the figure are discrete features that have both positive and negative frequency drifts. These features are similar to those discussed in the past by Gurnett et al. [1979c] and Benson et al. [1988b]. In addition, indicated on the plot is a narrow (in time) feature with negative slope extending from about 65 kHz down to about 40 kHz. We refer to this discrete feature as a stripe. It is not clear on this figure whether there is any curvature at the highest or lowest frequencies of the feature. Other examples do seem to indicate some curvature, particularly at the lowest frequency extent of the stripe. These signatures are not unique, and appear at other times in the Galileo wideband data as shown in Figure 3 for a time period about 20 minutes later. The features are observed near the end of the time interval extending over a frequency range 40 kHz $< f <$ 90 kHz. The features are not unique to the Galileo data. In Figure 4 we display wideband data obtained from the Plasma Wave Instrument on board the DE-1 spacecraft as it approached a source region of intense AKR in the midaltitude, evening-sector auroral region. Similar features are observed near the end of the spectrogram in the frequency range from about 100 kHz down to about 65 kHz. The slope is about the same, within a factor of 2.

In addition to DE-1 and Galileo, recent observations from Polar have also revealed AKR stripes in similar frequency range when the spacecraft was over the polar cap and well above the AKR source region. Figure 5 is an example of data obtained on March 28, 1996 when Polar was located approximately at r = 8.36 R_E, MLT = 01 hours, and L $>$ 100 (over the polar cap). The stripes are seen in the frequency range from about 65 kHz to perhaps over 90 kHz, although the upper frequency cutoff is not clear since the data is instrumentally restricted by the operating mode to frequencies less than 90 kHz. These stripes have a signature very similar to those observed both on Galileo and on DE-1. A typical slope was -5 kHz/sec. On March 13, 1996, Polar was again over the North polar

cap when the data of Figure 6 was taken. Here we see a large number of relatively intense stripes that are similar in morphology to those seen in Figure 5 except for number and intensity. However, in addition to the negative-slope stripes a few positive-slope stripes are also seen early in the plot (one is indicated with an arrow). These are the only observations of AKR stripes with a positive slope to date. The positive-slope stripes have a smaller extent in time and a larger slope, a typical value being about 15 kHz/sec.

In Table 1 we have summarized some typical data taken by all three satellites. For the negative-slope stripes we find the frequency extent ranges from 38 kHz to greater than 100 kHz and the frequency extent varies from less than 10 kHz to almost 30 kHz. The negative drift rates range from −9.0 kHz/sec to −4.6 kHz/sec. The total time extent of the drifts ranges from 1.9 to 4.8 seconds. Since the positive-slope stripes are the only cases we have yet observed, we cannot say that the numbers are typical, but it is clear that the drift rates are larger in magnitude and the time extents are relatively much shorter.

Table 1: Examples of AKR Stripes

Satellite	f_{min} (kHz)	f_{max} (kHz)	Slope (kHz/s)	Δt (sec)	Δf (kHz)	X* (R_E)	Y* (R_E)	Z* (R_E)
Galileo	38	65	−9.0	3.2	27	−8.86	6.72	3.39
Galileo	58	70	−6.0	2.1	12	−7.30	5.85	2.81
						r (R_E)	MLAT (deg)	MLT (hrs)
DE-1	88	97	−4.6	2.2	9	3.18	66.5	20.8
DE-1	88	99	−4.8	1.9	11	3.18	66.5	20.8
Polar	74	95	−4.8	4.5	21	8.36	L > 100	21.0
Polar	74	101	−5.3	4.8	27	8.36	L > 100	21.0
Polar	75	81	13.2	0.5	6	8.36	L > 100	21.0
Polar	71	78	18.9	0.4	7	8.36	L > 100	21.0

*GSE coordinates

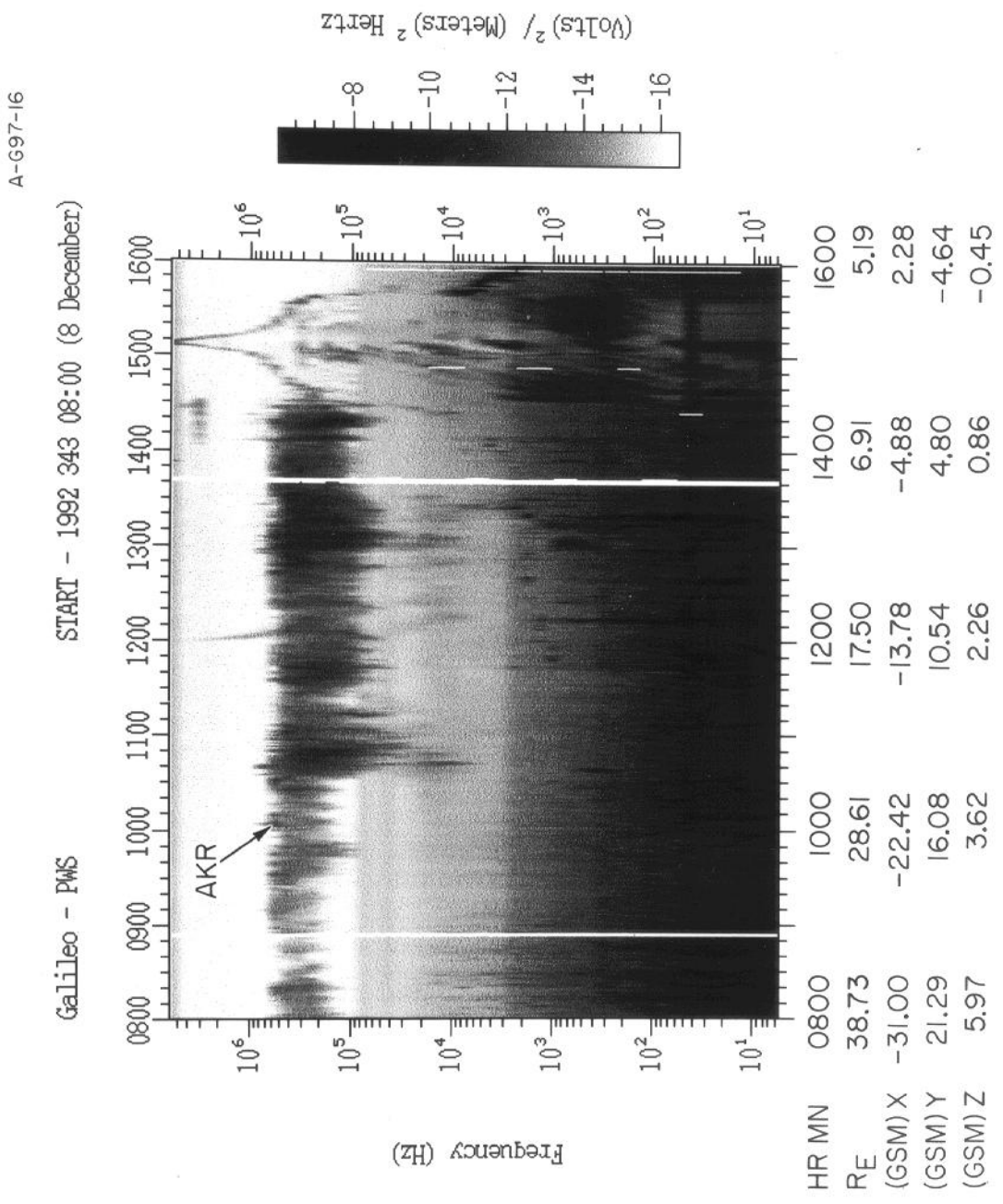

Figure 1: Seen is a frequency-versus-time color spectrogram with the wave intensity gray-coded. The frequency range extends from 1 Hz to 5.6 MHz on a log scale and includes emissions from the low, medium, and high frequency swept frequency receivers. The intense AKR is seen as black emission centered at about 200 kHz in the time range from 0800 to about 1430 UT. The closest approach (CA) is identified by the peak in the narrowbanded upper hybrid frequency near the maximum frequency of the plot at approximately 1510 UT.

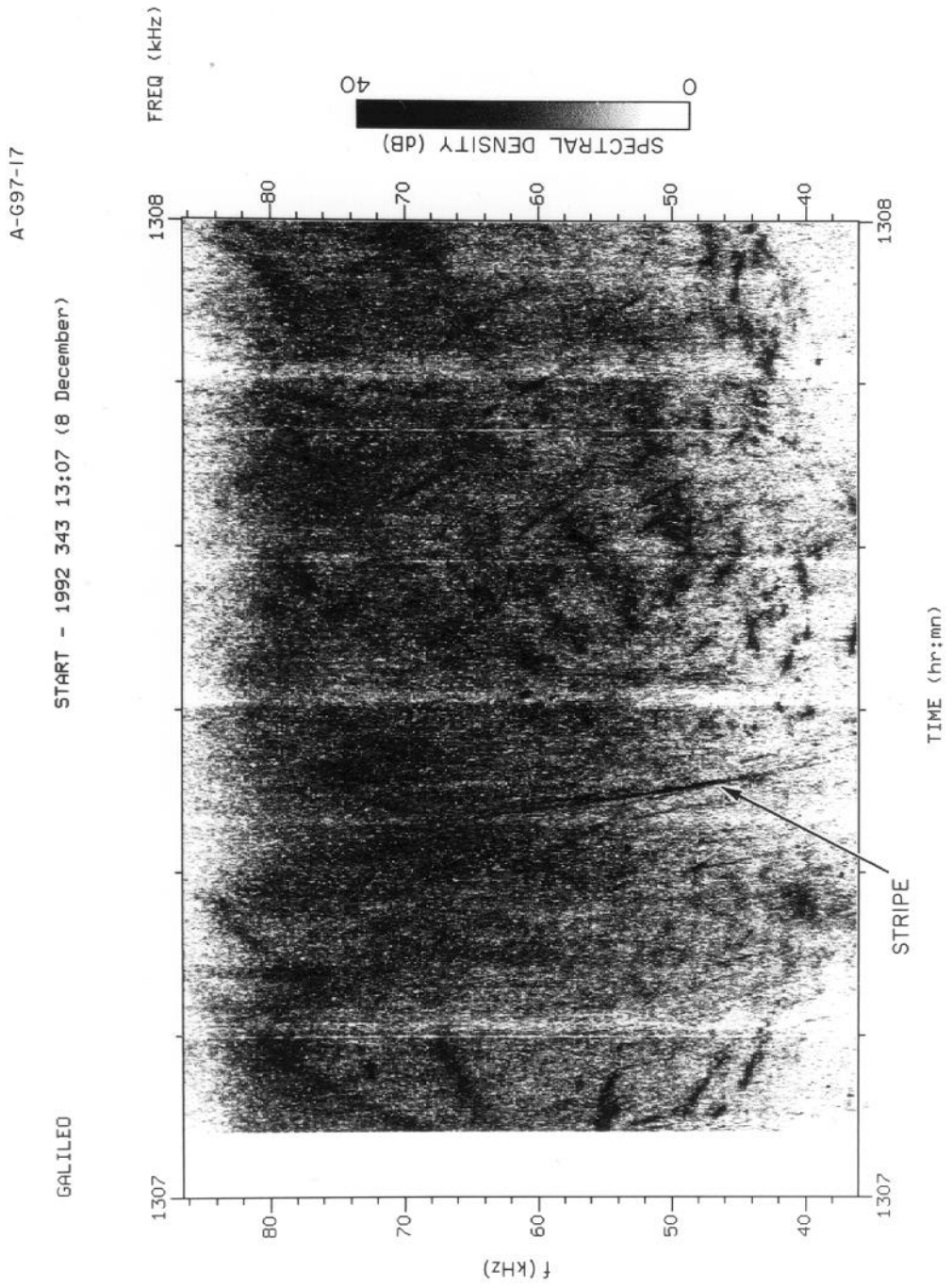

Figure 2: The wideband AKR data is plotted in a frequency-time spectrogram with the intensity gray-coded using a relative scale. The frequency range is from 40 to 80 kHz on a linear scale. The plot starts at 1307:04 and extends for 1 minute. The fine-structure is visible as dark positive and negative slope features. Note the discrete negative-slope feature referred to as a stripe and indicated by the arrow.

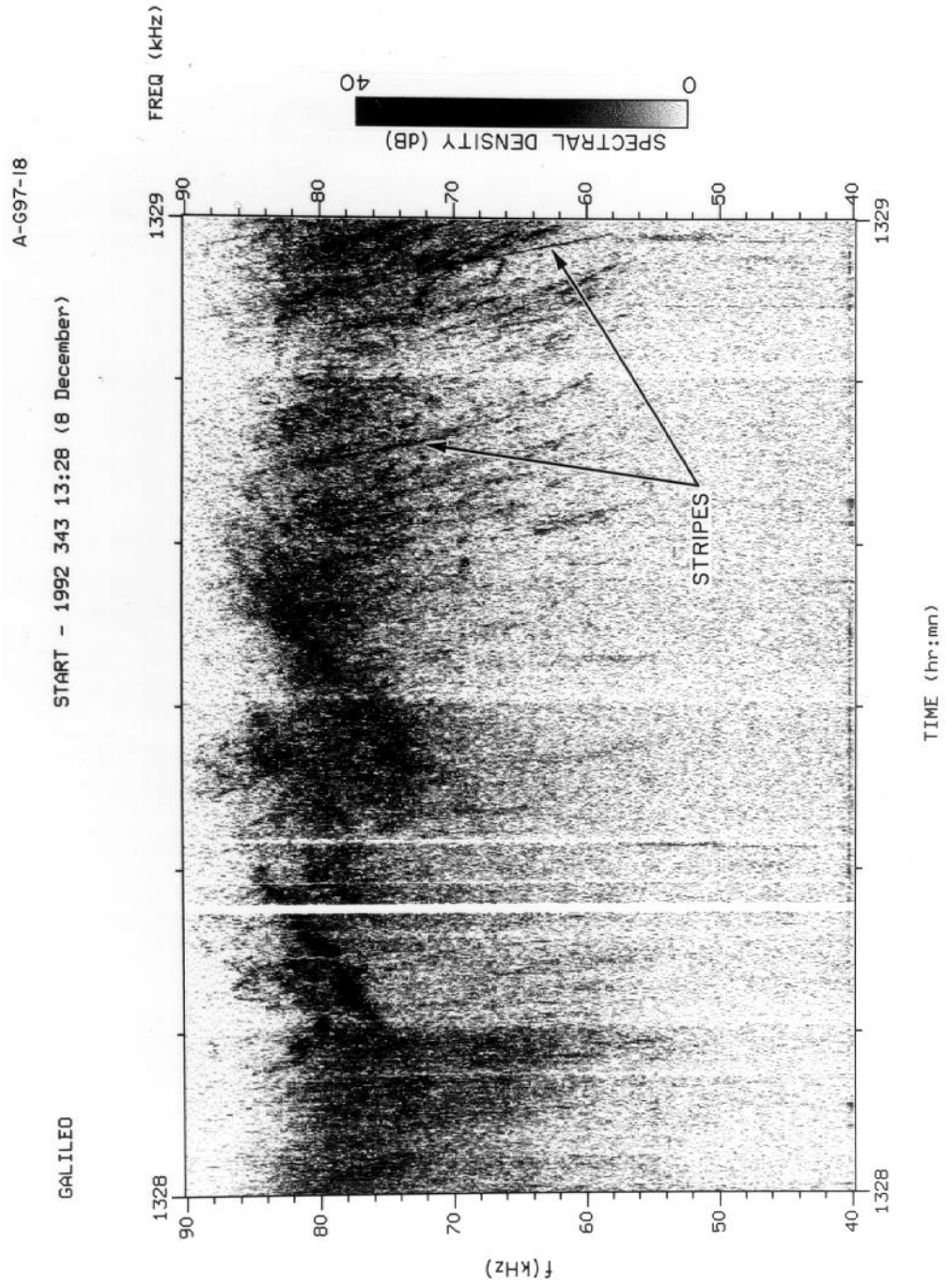

Figure 3: A wideband frequency-versus-time spectrogram of AKR for a period of time about 20 minutes later than the observations shown in Figure 2. The frequency range is linear from 40 kHz to 90 kHz, and the time extent of the plot is 1 minute. The discrete, negative-slope features (similar to Figure 2) are seen more clearly toward the end of the plot.

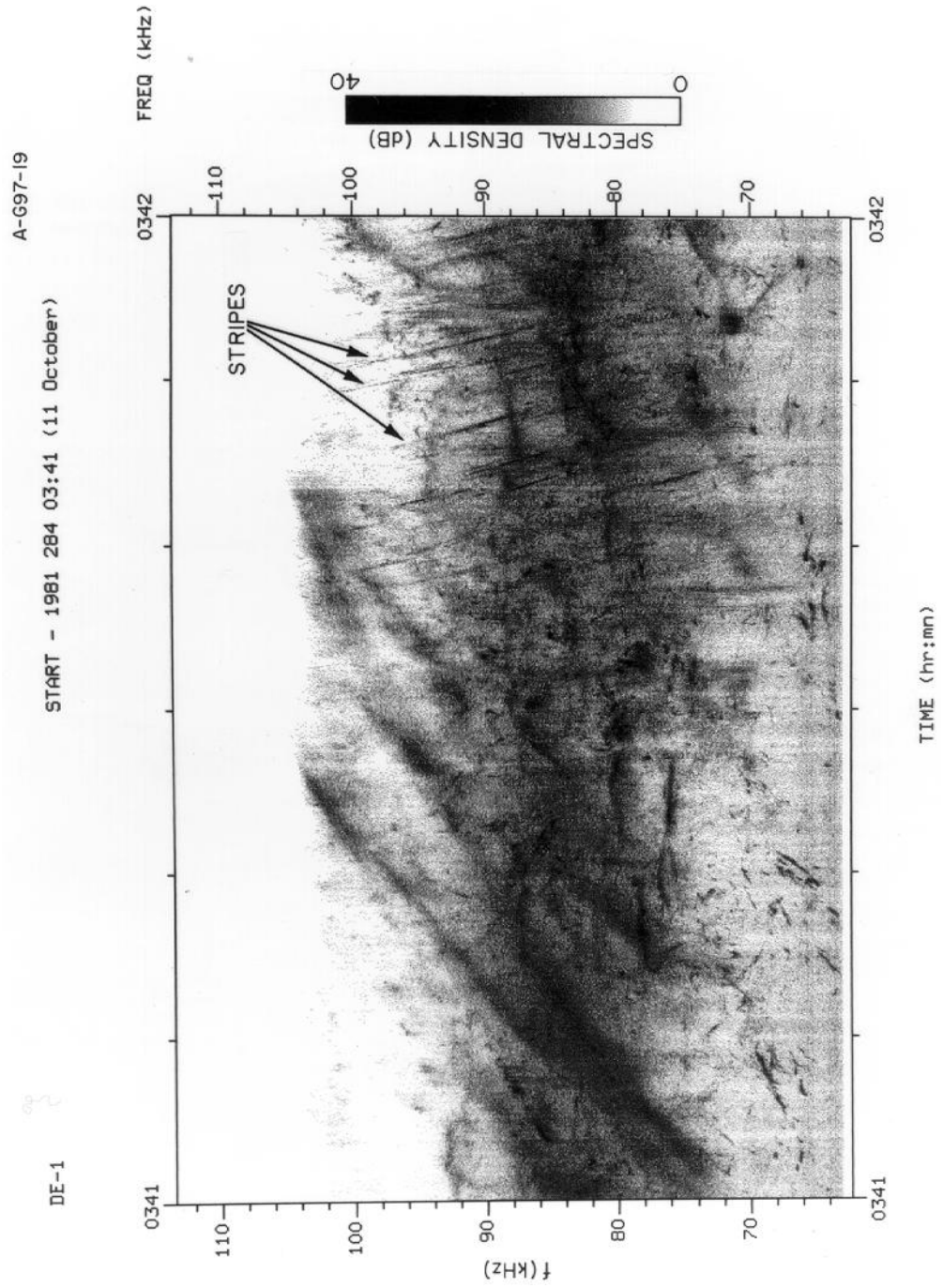

Figure 4: Wideband data obtained by the plasma wave instrument on board DE-1 as it approached the AKR source region in the mid-altitude nightside auroral region. The frequency scale is in kHz and the time extent is 1 minute. Again, the intensity scale is relative. Seen on the plot are large positive slope frequency drifting features, but also the discrete, negative-slope features (similar to Figures 2 and 3) more clearly visible in the last half of the plot.

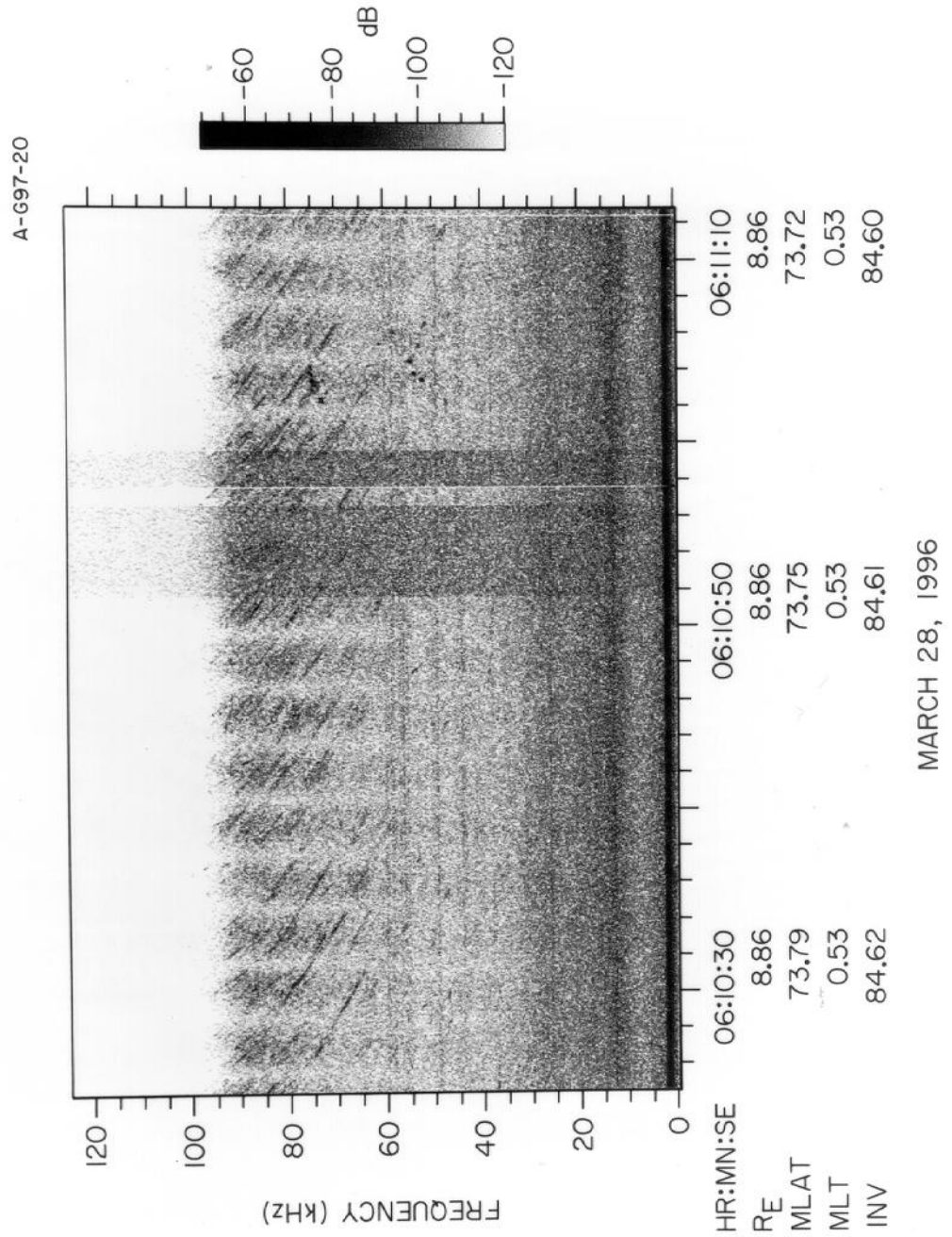

Figure 5: Wideband data obtained from the plasma wave instrument on board Polar as it was high over the northern polar cap on March 28, 1996 near r = 8.78 R_E, magnetic local time (MLT) = 0.49 hours and invariant latitude (IL) greater than 100. Note the numerous examples of negative-slope stripes observed in the frequency range from 60 kHz < f < 90 kHz.

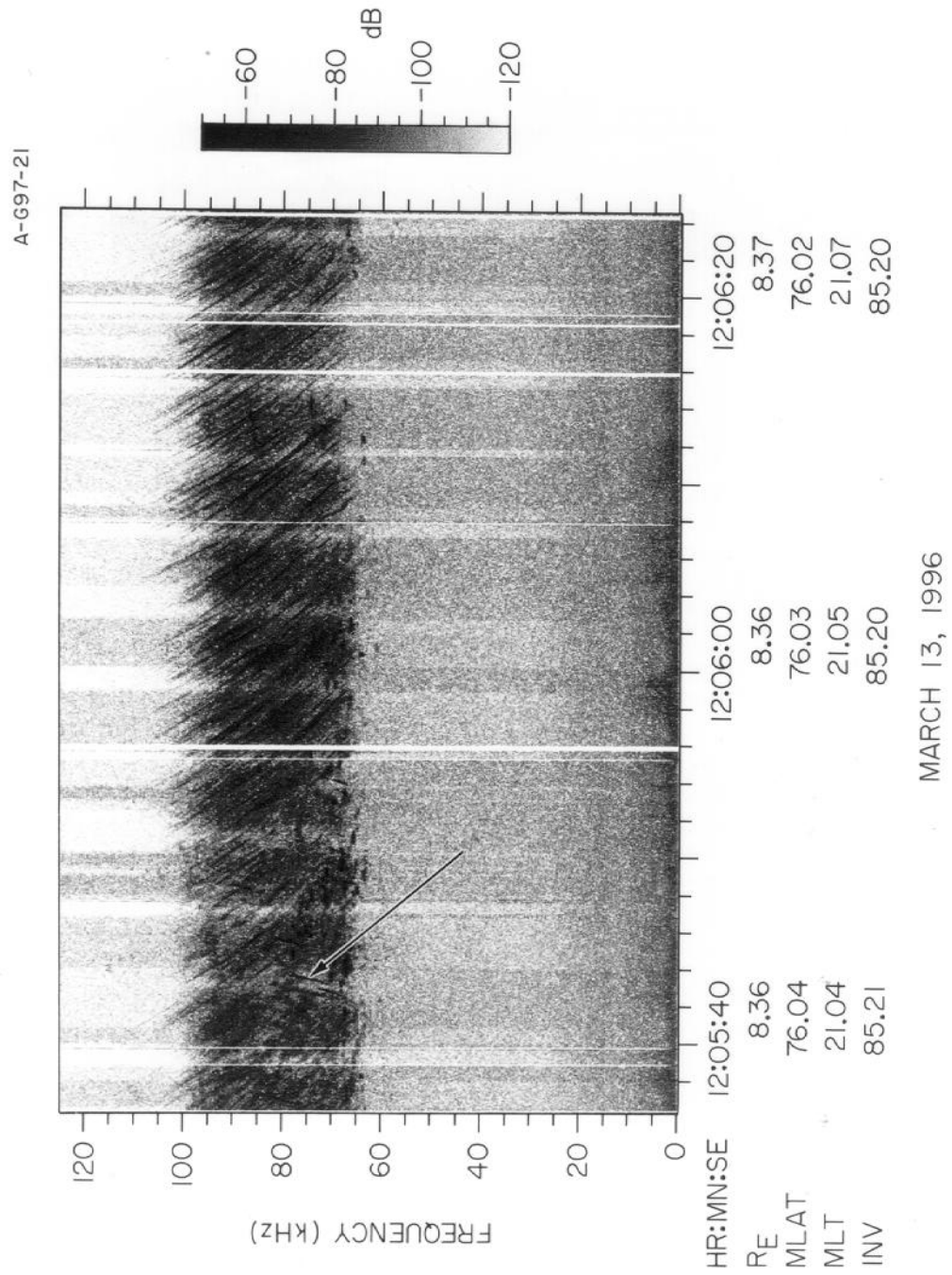

Figure 6: Wideband data obtained from the plasma wave instrument on board Polar as it was high over the northern polar cap on March 13, 1996 near $r = 8.36$ R_E, *MLT* $= 21.0$ *hours and invariant latitude greater than 100. Note the numerous and quite intense examples of negative-slope stripes observed in the frequency range from 60 kHz* $< f <$ *90 kHz. Also the arrow indicates one of several examples of rare positive-slope stripes. It is not yet known how common stripes of either slope are in higher frequency ranges of AKR.*

3 Analysis

Because of its isolated nature and relatively large frequency extent, Menietti et al. [1996] chose the signature indicated in Figure 2 for detailed study. They found the data points of this signature best fit a linear function with a slope of about -9 kHz/sec, as shown in their Figure 6. Menietti et al. [1996] considered two possible generation mechanisms: 1) possible impulsive stimulation of the entire AKR source region along a field line; 2) stimulated emission by a wave travelling up the magnetic field line.

In the first scenario, the signature was considered to be produced by an intrinsic dispersion due to the source mechanism. For gyroemission, the wave group velocity, V_g, decreases as the wave frequency approaches the local electron gyrofrequency, Ω_{ce}, and the group velocity decreases as the gyrofrequency decreases. The authors first considered the possibility of impulsively stimulated emission at frequencies very near Ω_{ce} at different points along the field line. They envisioned AKR generated with maximum growth rate at a frequency close to Ω_{ce} such that $V_g/c \ll 1$. We refer the reader to that study for details. The authors concluded that impulsive stimulation by intrinsic dispersion of the wave group velocity along the field line was not feasible for a number of reasons: 1) the calculated dispersion was not linear in disagreement with the observations; 2) the calculated dispersion curve required that the source region (where the plasma parameters would be applicable) be unphysically large (~ 10 R_E in diameter); 3) the calculated frequency dispersion was strongly dependent on local plasma parameters. For all of these reasons the authors concluded that intrinsic dispersion was not the mechanism responsible for the observed signatures in the AKR fine structure spectrum.

4 Wave Stimulation

The frequency extent of the assumed gyroemission observed in Figure 2 requires that the source region extends several thousand kilometers along the field line. The observed signature lasts about 3.5 seconds, so the stimulating wave must have a group velocity along the field line of about 1000 km/sec. The stripes for the observations made by DE-1 and Polar would require similar group velocities within a factor of 2 or 3. There are a number of candidates for such waves that have been observed regularly at frequencies near and below both the hydrogen and oxygen ion cyclotron frequencies [cf. Gurnett et al. 1984]. Menietti et al. [1996] showed how at mid-auroral altitudes the most likely candidate for waves with group velocities in the correct range is the EMIC wave.

In order to produce the negative slope of the stripe it is necessary that the wave travels up the field line from larger to smaller gyrofrequencies. Lin et al. [1989] have shown that auroral electron beams with energies of several keV are likely sources of free energy for EMIC waves generated along auroral field lines. Since the generation mechanism is Landau resonance, the direction of propagation of the waves depends on the direction of the electron beams. As shown in their Figures 4-6 for plasma parameters observed by DE-1 in the boundary plasma sheet (their Table 1), EM hydrogen and oxygen ion cyclotron waves are expected to have maximum growth rate in the frequency range $0.25\ \Omega_i \leq \omega \leq 0.9\Omega_i$,

where Ω_i is the ion cyclotron frequency. EMIC waves could propagate up the field line until they reached Ω_i where propagation would cease, and waves could propagate down the field line to the ionosphere and reflect at the point where the density gradient becomes very large (at altitudes of several hundred kilometers) [cf. Temerin et al. 1986].

Depicted in the cartoon of Figure 7 is a source of EMIC waves within the AKR source region. As mentioned above, the EMIC waves are envisioned to be generated by field-aligned electron beams, which are produced by the field-aligned electric field. Temerin et al. [1986] have argued that the source of EMIC waves responsible for the flickering aurora is located near the bottom of the acceleration region where one would expect to find precipitating electron beams necessary to satisfy the cyclotron resonance condition for downward propagating EMIC waves. In the case depicted in Figure 7, upward propagating EMIC waves are seen near the top of the acceleration region, in the lower-frequency AKR source region. This is required by the observations which show that the AKR stripes are observed in the lower frequency range of the AKR for $f < 100$ kHz. These waves might then stimulate the growth of AKR.

5 Discussion

The best examples of stripes to date occur when DE-1 and Polar are located in the polar cap and when the AKR is not so intense. If the AKR emission is intense, the stripes are washed out and not easily discerned. All of the observations occur at satellite altitudes that are greater than 2 R_E. This is higher than the postulated source altitude of AKR (~ 1 R_E). AKR observed at these high altitudes must be propagating upward from the source region and it is consistent with the cyclotron maser mechanism [Wu and Lee, 1979] to assume that the free-energy source of this emission is an upward loss cone electron population. Upward electron beams such as those that could excite upward propagating EMIC waves are often observed in the presence of upward loss cone populations in the auroral zone [cf. Lin et al. 1989]. We also note that Temerin et al. [1986, 1993] have modeled flickering aurora showing the correlation of electron data with standing EMIC waves. These waves probably have sources near the bottom of or just below the acceleration region at frequencies near or below the ion cyclotron frequency and propagate downward to reflect near the ion-hybrid frequency. Such observations would be consistent with our model of upward propagating EMIC waves that penetrate the acceleration region after reflection, for example. In this scenario it would be necessary for the bottom of the acceleration region to extend below the altitude of the ion cyclotron frequency.

The stripes have been observed occasionally in the Galileo and DE-1 data, but appear more frequently in the Polar data. It will be important to continue analysis of these emissions to determine the statistics of the frequency of occurrence, range of frequency, differences in drift rate, etc. If the scenario of wave-stimulated AKR is correct, we expect to find positive-slope stripes in the higher frequency wideband AKR data. Sources of higher frequency AKR occur at lower altitudes, within and beneath the acceleration region where downward electron beams are more common. Such downward electron beams are postulated to generate downward EMIC waves [cf. Temerin et al. 1986] and thus may stimulate discrete, positive-slope AKR stripes. We note that Shepherd et al. [this volume]

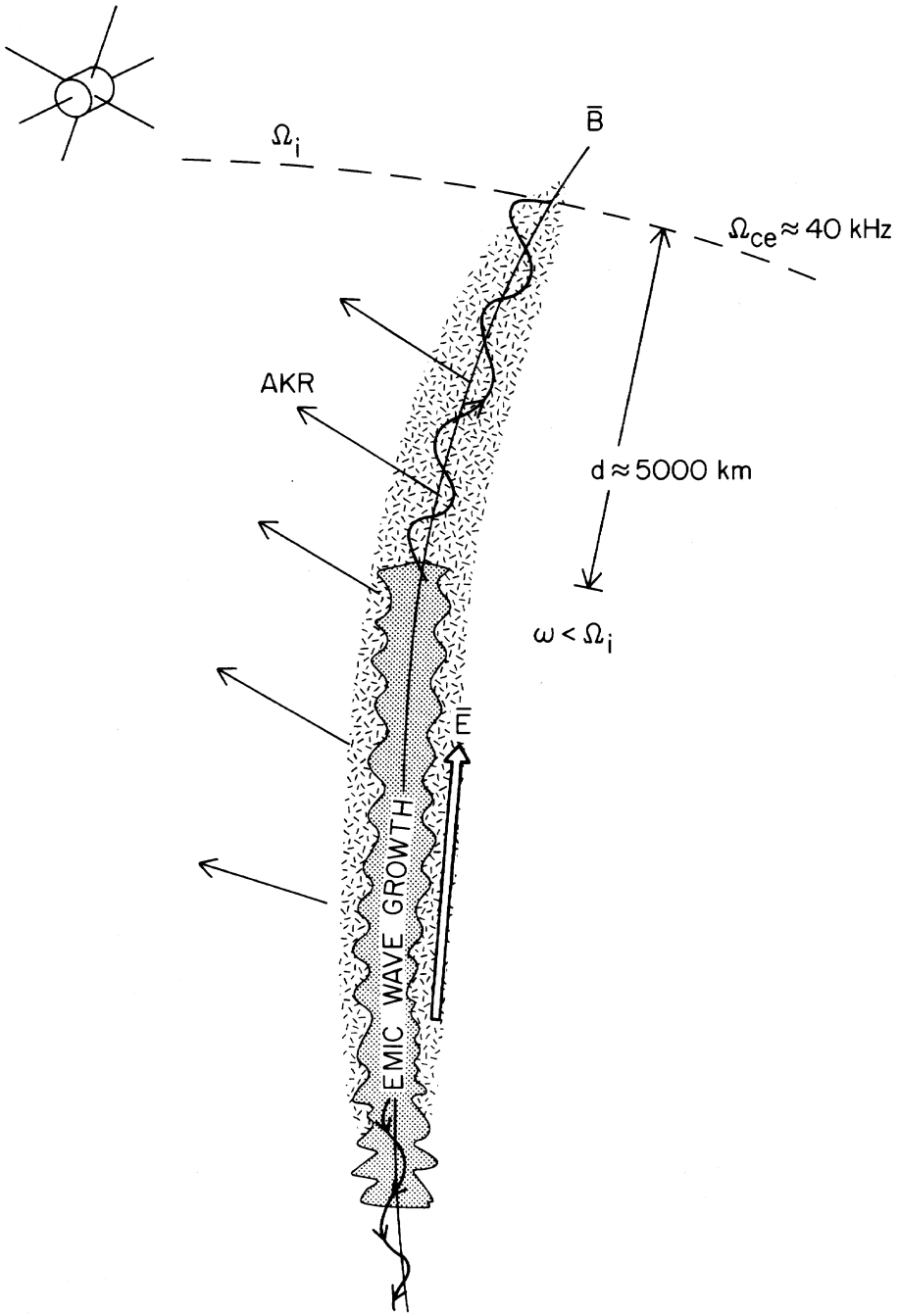

Figure 7: In this cartoon we depict an AKR source region being stimulated by a field-aligned wave travelling up the magnetic field line. EMIC waves are seen propagating near the top of the AKR source region, where the source of AKR for $f < 100$ kHz is located. For a total distance, d, of about 3000 km, the wave group velocity would have to be about 950 km/sec to produce a discrete feature that persists for about 3.5 seconds as observed. EMIC waves can propagate up the field line until they encounter Ω_i, or down the field line until they reach the ion hybrid resonance frequency deep in the ionosphere.

have identified positive-slope stripes in auroral roar emissions. These observations were made at frequencies in the range of several megahertz from ground-based radio receivers located beneath auroral features. It is tempting to suggest that such observations are in fact stimulated by downward propagating waves (such as EMIC waves) traversing the roar source region. We conclude that the data suggests that AKR may have both spontaneous and stimulated generation mechanisms.

We do not rule out the possibility that the stripes may be generated by upward electron beams or "individual isolated bunches of particles" as has recently been proposed by Carr et al. [this volume] for the generation of Jovian S-bursts. Similarly, as recently proposed by Zarka et al. [this volume] for the generation of Jovian S-bursts, the emission may be the result of generation regions that are in a "charged state" awaiting a stimulus from a passing beam. In the scenario we propose, the stimulus is a wave rather than a plasma beam or bundle.

6 Summary

Discrete "stripe-like" structures in the AKR wideband data are observed not infrequently in Galileo Earth flyby data and in the DE-1 and Polar auroral zone data. These signatures are characterized by the following features: $\Delta f \sim 30$ kHz, $\Delta t \leq 5$ seconds, dispersion fits a linear function. The stripes have been observed almost exclusively with negative slope at the lower range of AKR frequencies. A comprehensive study of the wideband AKR data at higher frequencies has not yet been conducted, however. To date, only a few cases of positive-slope stripes in the lower frequency wideband AKR data have been observed.

We suggest that the negative-slope stripes are produced by stimulation of the source region by electromagnetic plasma waves travelling away from Earth, through the AKR source region. A wave travelling up the magnetic field line with a group velocity of about 1000 km/sec would pass through the AKR source region (40 kHz $< f <$ 65 kHz) in about 3.5 seconds, in agreement with the typical observations. The source of the upward propagating EMIC waves may be near the top of the acceleration region where the local gyrofrequency is less than about 100 kHz. Alternatively, the EMIC source region could extend below the acceleration region in which case downward EMIC waves that subsequently reflect at low altitude to propagate back up through the AKR source region might be the source of the AKR stripes. Positive-slope stripes could be stimulated by downward propagating EMIC waves. These waves may be associated with AKR that propagates principally toward the Earth, and thus is not typically observed by a satellite above the AKR source region.

The actual mechanism by which the AKR emission is stimulated has not been critically investigated, but we suggest that as the stimulating wave propagates through the AKR source region, it modifies the ratio ω_p/Ω_{ce} and/or the plasma distribution in pitch angle or energy. As the time and frequency resolution of plasma wave receivers continues to increase we expect more revealing information relating to the details of plasma wave generation. We emphasize that the data presented in this work represent the results of

an investigation of only a small sampling of the available data from each of the three satellites. Examination of the Jupiter Galileo orbiter data has only just begun.

Acknowledgements: We have benefitted greatly from many discussions of these data with J. LaBelle and R. Treumann. We would like to thank K. Kurth for formatting the manuscript. The work of J.D.M. was funded by NASA contract 958779 with the Jet Propulsion Laboratory and by NASA contract NAS5–30371 with Goddard Space Flight Center. The research of H.K.W. was supported by NASA contract NAS5-32484 with USRA.